# Effect of Time-of-Flight Information on PET/MR Reconstruction Artifacts: Comparison of Free-breathing versus Breath-hold MR-based Attenuation Correction

Delso, Gaspar ; Khalighi, Mohammed ; Ter Voert, Edwin ; Barbosa, Felipe ; Sekine, Tetsuro ; Hüllner, Martin ; Veit-Haibach, Patrick

Abstract: Purpose To evaluate the magnitude and anatomic extent of the artifacts introduced on positron emission tomographic (PET)/magnetic resonance (MR) images by respiratory state mismatch in the attenuation map. Materials and Methods The method was tested on 14 patients referred for an oncologic examination who underwent PET/MR imaging. The acquisition included standard PET and MR series for each patient, and an additional attenuation correction series was acquired by using breath hold. PET data were reconstructed with and without time-of-flight (TOF) information, first by using the standard free-breathing attenuation map and then again by using the additional breath-hold map. Two-tailed paired t testing and linear regression with 0 intercept was performed on TOF versus non-TOF and free-breathing versus breath-hold data for all detected lesions. Results Fluorodeoxyglucose-avid lesions were found in eight of the 14 patients included in the study. The uptake differences (maximum standardized uptake values) between PET reconstructions with free-breathing versus breath-hold attenuation ranged, for non-TOF reconstructions, from -18% to 26%. The corresponding TOF reconstructions yielded differences from -15% to 18%. Conclusion TOF information was shown to reduce the artifacts caused at PET/MR by respiratory mismatch between emission and attenuation data. (©) RSNA, 2016 Online supplemental material is available for this article.

DOI: https://doi.org/10.1148/radiol.2016152509

Radiology



# Effect of Time-of-Flight Information on PET/MR Reconstruction Artifacts:

## Comparison of Free-breathing versus Breath-hold MR-based Attenuation Correction[1]

Gaspar Delso, PhD
Mohammed Khalighi, PhD
Edwin ter Voert, MS
Felipe Barbosa, MD
Tetsuro Sekine, MD, PhD
Martin Hüllner, MD
Patrick Veit-Haibach, MD

**Purpose:** To evaluate the magnitude and anatomic extent of the artifacts introduced on positron emission tomographic (PET)/magnetic resonance (MR) images by respiratory state mismatch in the attenuation map.

**Materials and Methods:** The method was tested on 14 patients referred for an oncologic examination who underwent PET/MR imaging. The acquisition included standard PET and MR series for each patient, and an additional attenuation correction series was acquired by using breath hold. PET data were reconstructed with and without time-of-flight (TOF) information, first by using the standard free-breathing attenuation map and then again by using the additional breath-hold map. Two-tailed paired *t* testing and linear regression with 0 intercept was performed on TOF versus non-TOF and free-breathing versus breath-hold data for all detected lesions.

**Results:** Fluorodeoxyglucose-avid lesions were found in eight of the 14 patients included in the study. The uptake differences (maximum standardized uptake values) between PET reconstructions with free-breathing versus breath-hold attenuation ranged, for non-TOF reconstructions, from −18% to 26%. The corresponding TOF reconstructions yielded differences from −15% to 18%.

**Conclusion:** TOF information was shown to reduce the artifacts caused at PET/MR by respiratory mismatch between emission and attenuation data.



*Online supplemental material is available for this article.*

[1] From the Applied Science Laboratory, GE Healthcare, Waukesha, Wis (G.D., M.K.); the Departments of Nuclear Medicine (E.t.V., F.B., T.S., M.H., P.V.H.), Neuroradiology (M.H.) and Medical Radiology (P.V.H.), University Hospital of Zurich; Department of Radiology, Nippon Medical School, Tokyo, Japan (T.S.); and University of Zurich, Zurich, Switzerland (E.t.V., M.H., P.V.H.). Received December 7, 2015; revision requested February 10, 2016; revision received March 10; accepted April 19; final version accepted May 3. **Address correspondence to** G.D., University Hospital of Zurich, Rämistrasse 100, Zurich 8006, Switzerland (e-mail: *gaspar.delso@ge.com*).

Supported by GE Healthcare (investigator-initiated research: PET/MR imaging clinical development—Lung lesions).

The latest generation of clinical positron emission tomography (PET)/magnetic resonance (MR) imagers introduces a new detector technology on the basis of silicon photomultipliers. This technology offers superior timing performance (1,2), which allows for time-of-flight (TOF) PET imaging.

TOF technology is not new or exclusive of PET/MR. Its effect on PET/computed tomographic (CT) imaging was thoroughly studied (3–6). It is known to provide an improvement of signal-to-noise ratio inversely proportional to the timing resolution of the system, which yields a better tradeoff between acquisition time, image noise, and structural contrast. It also improves imaging performance for heavier patients, which results in more uniform quality over all patient sizes.

However, a less known benefit of TOF makes it ideally suited for PET/MR imaging: Because TOF detectors narrow down the possible origin of positron emissions, the reconstruction becomes better conditioned and more likely to provide a globally optimal solution despite the presence of inaccuracies in the measured data and/or system model (7–9). In other words, PET becomes more robust to mistakes in the attenuation map. This property is of particular relevance in PET/MR imaging because MR-based attenuation correction is generally less accurate than its PET/CT counterpart (10–13). Not only are the attenuation coefficients a priori estimates rather than measurements, but there are also several sources of artifacts that can affect the attenuation map (14,15): field-of-view truncation, fat-water swaps, metal artifacts, and others.

For the particular case of the thorax, there is an intrinsic mismatch because of respiratory motion between PET emission data and the corresponding MR-based attenuation map. This study evaluates the magnitude and anatomic extent of the artifacts introduced in PET/MR images by respiratory state mismatch in the attenuation map.

## Advance in Knowledge

- Time-of-flight (TOF ) information was found to reduce the magnitude of respiratory mismatch artifacts from a range of −18% to 26% to a range of −15% to 18%.

## Materials and Methods

GE Healthcare (Waukesha, Wis) provided technical support for this study. Authors who are not employees of or consultants for GE Healthcare had control of inclusion of any data that might present a conflict of interest.

### Patient Population

Datasets from 14 patients from the nuclear medicine department were used in this study. Patients were included when they were suspected of having pulmonary lesions (benign or malignant) on the basis of the clinical indication or referral information and/or when patients had known lesions from previous imaging. All patients were included consecutively. No patients were excluded from this consecutive series.

The patient population consisted of 10 men (mean age ± standard deviation, 64 years ± 11; range, 36–79 years) and four women (mean age, 64 years ± 3; range, 58–67 years). Student *t* test revealed no statistically significant difference between these group averages. The average population age was 64 years ± 10 (age range, 36–79 years), weight was 75 kg ± 14 (range, 54–102 kg), and body mass index was 25.8 kg/m$^2$ ± 3.6 (range, 21.5–35.7 kg/m$^2$). Patients were imaged with the same PET/MR imager (Signa PET/MR; GE Healthcare). This prospective study and data acquisition were approved by the local ethics committee, and all patients provided written informed consent before the examination. Eight of the 14 patients were included in a separate, as-yet-unpublished study. In our study, we report on the effect of respiratory motion and TOF on ungated datasets.

## Implication for Patient Care

- Our reported results demonstrated the benefit of TOF reconstruction for the minimization of the residual misalignment artifacts.

### Data Acquisition

All patients were injected an average dose of 3.3 MBq/kg ± 0.3 (range, 3.0–3.8 MBq/kg) fluorine 18 fluorodeoxyglucose (FDG). An uptake time of approximately 40 minutes was allowed before the patients underwent a PET/MR examination, and the protocol was set up so that the PET acquisition would start after 60 minutes of uptake time.

The acquisition protocol varied depending on the indication, including both single and multibed examinations with PET acquisition times ranging from 2 to 8 minutes per bed position (eg, depending on the presence or absence of triggered MR sequences). Clinical MR sequences were performed simultaneously with each PET bed and with an automated attenuation correction sequence (Lava Flex, GE Healthcare; dual-echo spoiled gradient-recalled acquisition in the steady state; 256 × 128 × 120 matrix; 1.95 × 1.95 × 2.6 mm$^3$ resolution; imaging time, 18 seconds). This sequence was by default performed during free breathing.

In each patient, after completion of the PET task in the thorax, the examination was repeated with the same geometrical settings, instructing the patient to perform an end-expiratory breath

**Published online before print**
10.1148/radiol.2016152509 **Content code:** MR

**Radiology 2016;** 000:1–7

**Abbreviations:**
FDG = fluorodeoxyglucose
TOF = time of flight

**Author contributions:**
Guarantors of integrity of entire study, G.D., F.B.; study concepts/study design or data acquisition or data analysis/interpretation, all authors; manuscript drafting or manuscript revision for important intellectual content, all authors; approval of final version of submitted manuscript, all authors; agrees to ensure any questions related to the work are appropriately resolved, all authors; literature research, G.D., E.t.V., F.B., M.H., P.V.H.; clinical studies, G.D., M.K., E.t.V., F.B., M.H., P.V.H.; experimental studies, E.t.V.; statistical analysis, G.D.; and manuscript editing, all authors

Conflicts of interest are listed at the end of this article.

**Figure 1**

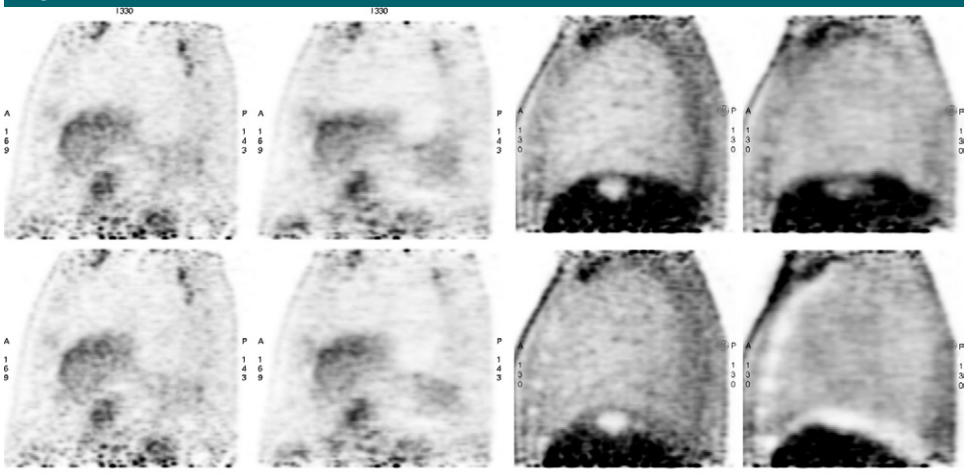


**Figure 1:** Sagittal PET images in two patients. **(a)** Images in patient 2 show one of the FDG-avid pleural lesions. **(b)** Images in patient 8 show the FDG-negative lesion in the apex of the liver. The top row shows reconstructions that use free-breathing attenuation correction data, the bottom row shows reconstructions that use breath-hold attenuation correction data (inspiratory breath hold). The views on the left column were reconstructed by using TOF information and the views on the right were reconstructed without TOF information.

hold (ie, "please breathe in… breathe out… hold your breath") during the attenuation correction sequence. PET data from this second acquisition were discarded.

### Data Processing

PET images were reconstructed for the bed positions that covered the thorax by using a three-dimensional ordered-subset expectation maximization method (VuePoint HD; GE Healthcare) with four iterations and 28 subsets onto a $256 \times 256 \times 89$ matrix with voxel size of $2.34 \times 2.34 \times 2.78$ $mm^3$. The reconstructed images were filtered by using a transaxial Gaussian filter (5-mm full width at half maximum) followed by a three-section axial filter (ratio of 1:4:1). Quantitative corrections applied during image reconstruction included normalization, dead time, point-spread function, randoms, scatter, decay, and attenuation. The latter was based on a four-tissue-class (air, lung, fat, and soft tissue) segmented attenuation map, automatically generated from the results of the MR-based attenuation correction acquisition (Lava Flex; GE Healthcare) (13). The attenuation coefficients for air (0 $cm^{-1}$) and lungs (0.018 $cm^{-1}$) are fixed, whereas those of other tissues were a weighted average of their fat (0.086 $cm^{-1}$) and soft tissue (0.100 $cm^{-1}$) composition. Patient tissue outside the 50-cm field of view (Lava Flex) was automatically identified from a non-attenuation-corrected PET reconstruction and assigned soft tissue-equivalent attenuation.

A second PET reconstruction examination was performed in each patient (ie, free-breathing and breath-hold MR-based attenuation correction), this time by using a three-dimensional algorithm (Osem; VuePoint FX) that took into account the TOF information to take advantage of the less-than-400-picosecond timing resolution of the detectors (16).

### Statistical Methods

Parameters obtained from lesions (size, maximum standardized uptake value, and mean standardized uptake value) were analyzed by using software (Prism, Graphpad Software, La Jolla, Calif; and Excel, Microsoft, Redmond, Wash). Two-tailed paired $t$ testing and linear regression with 0 intercept was performed on TOF versus non-TOF and free-breathing versus breath-hold data.

## Results

The reconstructed PET emission images (Fig E1 [online]) were analyzed by two radiologists (F.B. and T.S., with 7 and 10 years of experience, respectively) and one radiologist and nuclear medicine physician (M.H., with 8 years of experience) by using a work station (Advantage Workstation; GE Healthcare) with the standard clinical oncology review protocol. FDG-avid lesions were found in eight of the 14 patients included in the study, five of the remaining patients showed no noticeable lesions, and one patient presented with a lesion that was not FDG avid (ie, cyst or hemangioma) in the liver. Figure 1 includes the reconstructed PET emission data for this FDG-negative lesion, including free-breathing and breath-hold attenuation correction data. A summary of all encountered lesions is included in Table E1 (online).

Three of the 14 patients (patients 1, 8, and 10) were found to have performed an inspiratory breath hold rather than the nonforced end-expiration breath hold they were instructed to perform. This situation leads to much larger anatomic mismatch between the MR and PET datasets. These patients

**Table 1**

**Summary of Lesion Sizes and Uptakes, Measured with the Clinical Standard (ie, Free-Breathing) Datasets**

| Parameter | Non-TOF | TOF |
|---|---|---|
| All lesions | | |
| Size ($cm^3$) | 3.0 ± 2.5 | 2.1 ± 2.3 |
| $SUV_{max}$ | 4.8 ± 3.9 | 5.6 ± 4.1 |
| $SUV_{mean}$ | 2.9 ± 2.2 | 3.4 ± 2.2 |
| Small lesions | | |
| Size ($cm^3$) | 1.8 ± 0.7 | 0.9 ± 0.4 |
| $SUV_{max}$ | 4.9 ± 4.7 | 5.9 ± 4.8 |
| $SUV_{mean}$ | 3.0 ± 2.6 | 3.6 ± 2.6 |

Note.—Small lesions were considered to be lesions less than 2 $cm^3$. $SUV_{max}$ = maximum standardized uptake value, $SUV_{mean}$ = mean standardized uptake value.

were excluded from the subsequent analysis and studied separately.

The size and FDG uptake of each lesion were measured on the reconstructed PET emission datasets by using the auto-contour tool provided by the workstation (Advantage Workstation; GE Healthcare). Lesion sizes and uptakes on the clinical standard dataset (free-breathing MR-based attenuation correction, and TOF reconstruction) are summarized in Table 1. Non-TOF reconstructions yielded noticeably larger sizes and lower uptake (statistical significance confirmed by two-tailed paired $t$ test; $P < .01$). These differences were especially relevant for very small lesions (<2 $cm^3$).

Figure 2 shows the analysis of the scatterplots of the standardized uptake value of the lesions measured on TOF and non-TOF reconstructions. The value of each lesion is included twice, once measured on reconstructions by using free-breathing attenuation correction and once again measured on reconstructions by using breath hold. Both maximum and mean standardized uptake value plots showed good correlation between TOF and non-TOF values ($R^2 > 0.9$), and TOF uptake values had a trend that was approximately 10% higher than non-TOF uptake values.

The differences in maximum standardized uptake values between PET reconstructions with free-breathing versus breath-hold attenuation maps ranged from −15% to 18% for TOF reconstructions. The corresponding non-TOF reconstructions yielded differences from −18% to 26%. The mean standardized uptake value differences ranged from −14% to 16% for TOF and from −19% to 18% for non-TOF values. Table 2 summarizes these results. The statistical power was insufficient to determine the significance of these trends because of the reduced sample size with respect to all possible lesion placements and artifact configurations (paired $t$ testing; maximum and minimum standardized uptake value absolute differences, $P = .03$ and .08, respectively). Figure 2 also shows the scatterplot of the normalized differences between free-breathing and breath-hold MR-based attenuation correction.

The results of voxel-wise comparison between the different reconstructions are included as supplementary material (Figs E2–E5 [online]). The percent normalized error was used and presented as $\varepsilon = 100 \cdot (I_2 - I_1)/I_1$, where $I_1$ is the imager's original (ie, free-breathing) reconstruction and $I_2$ is the new (ie, breath-hold) reconstruction. Regions of low uptake (<500 Bq/mL) were excluded.

The distribution of the uptake differences between free-breathing and breath-hold MR-based attenuation correction reconstructions are presented in Figure 3a and 3b. Separate log-histograms are provided for end-expiration breath-hold and inspiratory breath-hold patients. A different representation of these same results can be found in Figure 3c and 3d, where cumulative distribution functions of the absolute uptake differences are shown. The presented graphs are the average of the individual curves measured for all patients. These differences indicate errors in the reconstructed PET uptake caused by anatomic mismatch in the attenuation maps; the figures show that, in TOF reconstructions, roughly 90% of the image voxels have absolute errors of 10% or less (an acceptable range for most clinical applications). In non-TOF reconstructions, only 82% of the image voxels are below 10% absolute error.

## Discussion

We compared the two MR-based attenuation correction options currently available for the thoracic region: free-breathing and breath-hold automated attenuation correction sequence (Lava Flex; GE Healthcare). Our patients were instructed to perform a standard, nonforced, end-expiration breath hold because it provides the closest approximation to the quiescent phase of the respiratory cycle. Three patients erroneously performed an inspiratory breath hold, which is known to lead to large anatomic mismatch. We include these results in a separate group because this is not an uncommon situation in clinical practice, especially in oncology where patients are usually elderly and compliance issues frequently arise.

Because of the lack of a standard reference, the difference between free-breathing and breath-hold MR-based attenuation correction was used as an estimate of the expected error range caused by respiratory mismatch. Notice that PET/CT data would still not constitute a standard of reference. Barring sophisticated approaches not used in clinical practice (eg, attenuation correction on the basis of dynamic CT) (17–20), there is no practical way to estimate patient attenuation in the presence of respiratory motion.

Voxel-wise maps offer the most intuitive representation of the bias that respiratory mismatch can introduce in PET (Figs E2–E5 [online]). Notice how normalized error values larger than ±10% can be found over the entire lung contour. These results agree with previously published PET/CT results (21). These results are particularly important for routine clinical reading. While the artifacts, for example, shown in Figure 1 can be readily identified as such, lesions of intermediate size can completely disappear and might therefore lead to a misdiagnosis. In case of follow-up studies, such errors can lead to misinterpretation because standardized uptake value measurements are likely to be inconsistent for lesions located in areas affected by respiratory mismatch. Such misinterpretation (ie, stable vs progressive or regressive

**Figure 2**

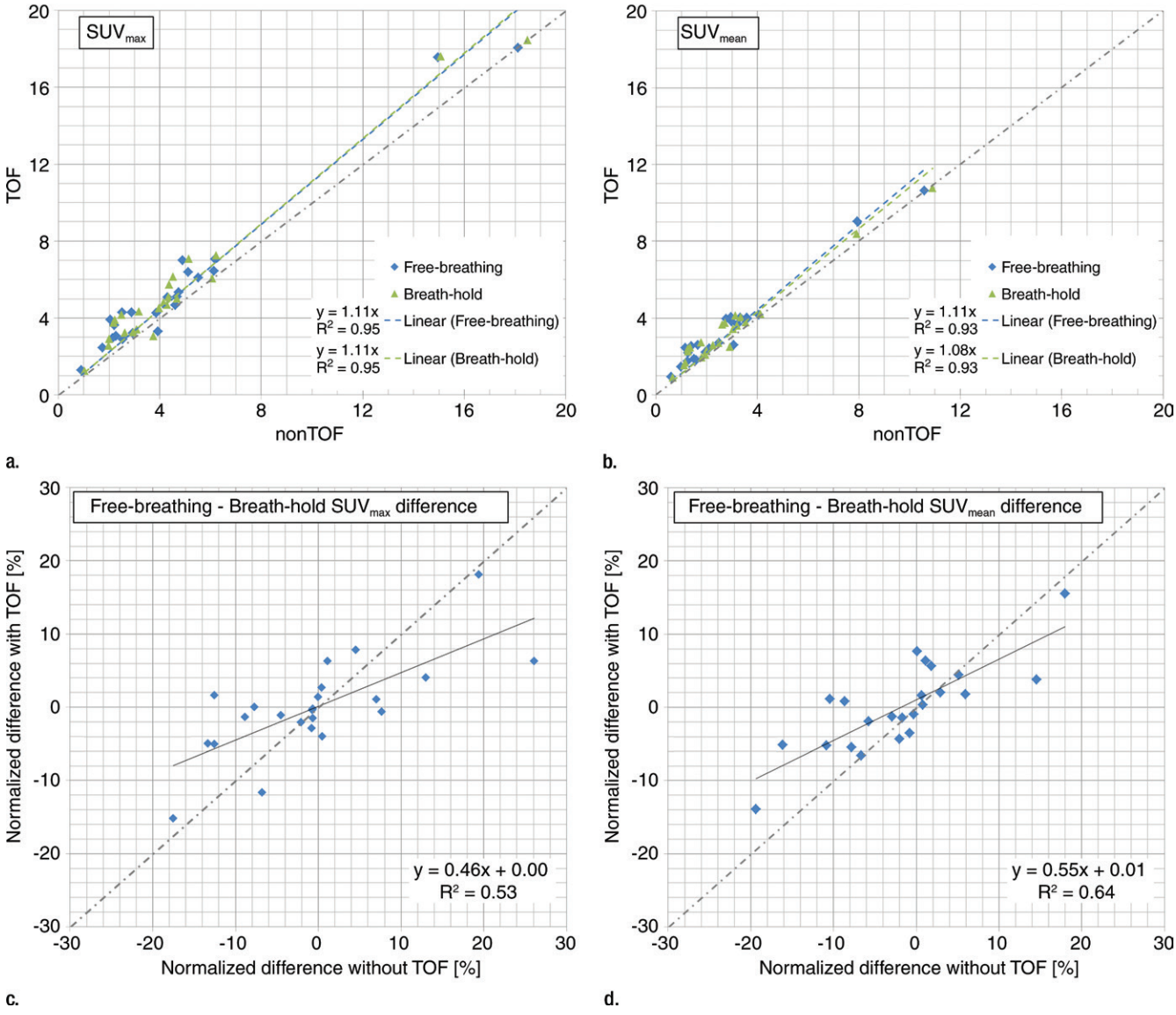


**Figure 2:** **(a, b)** Scatterplots of the maximum (**a**) and mean (**b**) standardized uptake ($SUV_{max}$ and $SUV_{mean}$, respectively) of the FDG-avid lesions found in the patients measured on TOF and non-TOF reconstructions. The value of each lesion is included twice, once measured on reconstructions by using free-breathing attenuation correction and once again measured on reconstructions by using breath-hold attenuation correction. **(c, d)** Scatterplots of the normalized differences between free-breathing and breath-hold attenuation of maximum (**c**) and mean (**d**) standardized uptake value. The regression line shows a slope smaller than 1, which suggests that TOF reconstruction provides more consistent results in the presence of attenuation map variation.

disease) can have an effect on the therapeutic management of patients. Overall, there might be a slightly increased risk of initial mischaracterization and misinterpretation of the effect of a therapy.

The effect of the use of TOF reconstruction is best appreciated in the error plot (Fig 3). The high error range is dominated by the non-TOF reconstruction, whereas small errors dominate in TOF reconstructions. This is also shown in the supplementary figures (Fig E1–E5 [online]), where TOF reconstructions show small magnitude errors spread over large areas, compared with non-TOF reconstructions that show errors of larger magnitude but over smaller areas. These results are consistent with previous findings (8,9,22,23) and are explained by the additional constraints imposed on the reconstruction by TOF information.

The decision regarding whether generalized small-magnitude errors are preferable to localized large-magnitude ones belongs to the clinician on the basis of the needs of each clinical application. For the particular case of oncologic

**Table 2**

**Summary of Lesion Uptake Differences between PET Reconstructions with Free-breathing and Breath-hold Attenuation Correction**

| | Normalized Error | | Absolute Normalized Error* | |
|---|---|---|---|---|
| Parameter | Non-TOF | TOF | Non-TOF | TOF |
| $SUV_{max}$ | 0 ± 10 | 0 ± 6 | 7 ± 7 | 4 ± 5 |
| $SUV_{mean}$ | −2 ± 8 | 0 ± 6 | 6 ± 6 | 4 ± 4 |

Note.—Data are percentages. These values constitute an estimate of the expected error ranges caused by respiratory mismatch. $SUV_{max}$ = maximum standardized uptake value, $SUV_{mean}$ = mean standardized uptake value.

* Significantly different: maximum standardized uptake value, $P = .03$; mean standardized uptake value, $P = .08$.

staging, where uptake measurements of localized structures are sought, TOF information seems clearly advantageous. This is because the clinical influence of this effect is smaller because the magnitude of error itself is smaller and it affects the image more homogeneously.

The TOF property of robustness to inconsistencies between emission and attenuation data are of particular relevance for PET/MR imaging and needs revisiting within this new context. Indeed, the estimation of photon attenuation (both

**Figure 3**

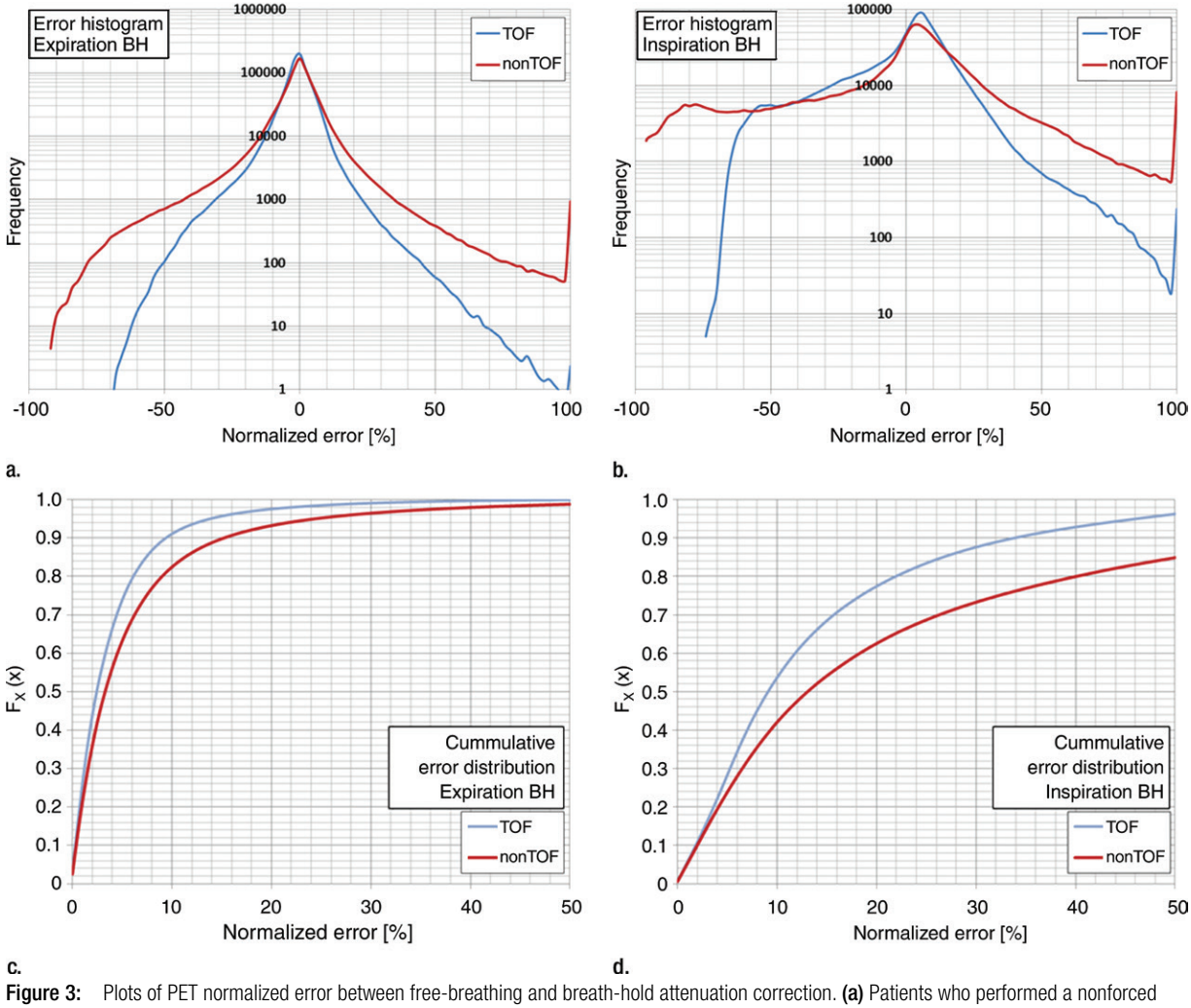


**Figure 3:** Plots of PET normalized error between free-breathing and breath-hold attenuation correction. **(a)** Patients who performed a nonforced expiratory breath hold (*BH*) during the acquisition of the attenuation correction MR sequence. **(b)** Patients who performed an inspiratory breath hold. The frequency axis (**a**, **b**) indicates the number of voxels affected by each error magnitude (in logarithmic scale). **(c**, **d)** Cumulative distribution functions of the absolute normalized PET error, averaged over all patients: **(c)** nonforced expiratory breath hold and **(d)** inspiratory breath hold.

caused by patient tissue and MR hardware) from MR data is a well-known challenge. PET/MR attenuation maps are generally less accurate than PET/CT (see Fig E1 [online]) and are prone to artifacts (eg, motion, metallic implants, and truncation). For the particular case of the thorax, PET emission data will (in the absence of gating) be an average of all respiratory states, whereas respiratory motion in MR causes ghosting artifacts rather than averaging.

The main limitations of this study were the reduced patient population, which prevented a stratified statistical analysis of the artifacts, and the absence of gated reconstructions in the comparison. Ongoing work is aimed at extending this study to gated PET acquisitions, where both the negative effect of anatomical misalignment and the benefit of breath-hold attenuation correction are expected to be more noticeable. In particular, it would be of interest to evaluate the effect of TOF in patients with very shallow or irregular breathing patterns (common in certain clinical indications), where the accuracy of gating and motion correction approaches may be limited.

The results presented here support the premise that TOF reconstruction mitigates the errors introduced in reconstructed PET images by respiratory state mismatch in the attenuation map (maximum standardized uptake value errors ranged from −18% to 26% for non-TOF and from −15% to 18% for TOF). These errors were confirmed to exceed the clinically acceptable range, not only in the vicinity of the diaphragm but all over the lung contour.

**Disclosures of Conflicts of Interest: G.D.** Activities related to the present article: disclosed no relevant relationships. Activities not related to the present article: author is an employee of GE Healthcare. Other relationships: disclosed no relevant relationships. **M.K.** Activities related to the present article: disclosed no relevant relationships. Activities not related to the present article: author is an employee of GE Healthcare. Other relationships: disclosed no relevant relationships. **E.t.V.** Activities related to the present article: disclosed no relevant relationships. Activities not related to the present article: author received investigator-initiated study grants from Bayer Healthcare, Siemens Healthcare, and Roche Pharmaceuticals, and speaker fees from GE Healthcare. Other relationships: disclosed no relevant relationships. **F.B.** disclosed no relevant relationships. **T.S.** disclosed no relevant relationships. **M.H.** Activities related to the present article: disclosed no relevant relationships. Activities not related to the present article: author disclosed personal fees from GE Healthcare and from Mepha. Other relationships: disclosed no relevant relationships. **P.V.H.** Activities related to the present article: disclosed no relevant relationships. Activities not related to the present article: author disclosed grants from GE Healthcare, Roche Pharmaceuticals, and Bayer Healthcare, and personal fees from GE Healthcare. Other relationships: disclosed no relevant relationships.

## References

1. Del Guerra A, Belcari N, Bisogni MG, et al. Silicon Photomultipliers (SiPM) as novel photodetectors for PET. Nucl Instrum Methods Phys Res A 2011;648(Supplement 1):S232–S235.
2. Zaidi H, Del Guerra A. An outlook on future design of hybrid PET/MRI systems. Med Phys 2011;38(10):5667–5689.
3. Kadrmas DJ, Casey ME, Conti M, Jakoby BW, Lois C, Townsend DW. Impact of time-of-flight on PET tumor detection. J Nucl Med 2009;50(8):1315–1323.
4. Lois C, Jakoby BW, Long MJ, et al. An assessment of the impact of incorporating time-of-flight information into clinical PET/CT imaging. J Nucl Med 2010;51(2):237–245.
5. El Fakhri G, Surti S, Trott CM, Scheuermann J, Karp JS. Improvement in lesion detection with whole-body oncologic time-of-flight PET. J Nucl Med 2011;52(3):347–353.
6. Surti S. Update on time-of-flight PET imaging. J Nucl Med 2015;56(1):98–105.
7. Turkington TG, Wilson JM. Attenuation artifacts and time-of-flight PET. Presented at the 2009 IEEE Nuclear Science Symposium Conference Record (NSS/MIC), Orlando, Fla, October 24–November 1, 2009.
8. Davison H, ter Voert EE, de Galiza Barbosa F, Veit-Haibach P, Delso G. Incorporation of time-of-flight information reduces metal artifacts in simultaneous positron emission tomography/magnetic resonance imaging: a simulation study. Invest Radiol 2015;50(7):423–429.
9. Mehranian A, Zaidi H. Impact of time-of-flight PET on quantification errors in MR imaging-based attenuation correction. J Nucl Med 2015;56(4):635–641.
10. Vandenberghe S, Marsden PK. PET-MRI: a review of challenges and solutions in the development of integrated multimodality imaging. Phys Med Biol 2015;60(4):R115–R154.
11. Martinez-Möller A, Souvatzoglou M, Delso G, et al. Tissue classification as a potential approach for attenuation correction in whole-body PET/MRI: evaluation with PET/CT data. J Nucl Med 2009;50(4):520–526.
12. Schulz V, Torres-Espallardo I, Renisch S, et al. Automatic, three-segment, MR-based attenuation correction for whole-body PET/MR data. Eur J Nucl Med Mol Imaging 2011;38(1):138–152.
13. Wollenweber SD, Ambwani S, Lonn AH, et al. Comparison of 4-class and continuous fat/water methods for whole-body, MR-based PET attenuation correction. IEEE Trans Nucl Sci 2013;60(5):3391–3398.
14. Buchbender C, Hartung-Knemeyer V, Forsting M, Antoch G, Heusner TA. Positron emission tomography (PET) attenuation correction artefacts in PET/CT and PET/MRI. Br J Radiol 2013;86(1025):20120570.
15. Attenberger U, Catana C, Chandarana H, et al. Whole-body FDG PET-MR oncologic imaging: pitfalls in clinical interpretation related to inaccurate MR-based attenuation correction. Abdom Imaging 2015;40(6):1374–1386.
16. Levin C, Glover G, Deller T, McDaniel D, Peterson W, Maramraju SH. Prototype time-of-flight PET ring integrated with a 3T MRI system for simultaneous whole-body PET/MR imaging. J Nucl Med 2013;54(Supplement 2):148.
17. Pan T, Mawlawi O, Nehmeh SA, et al. Attenuation correction of PET images with respiration-averaged CT images in PET/CT. J Nucl Med 2005;46(9):1481–1487.
18. Alessio AM, Kohlmyer S, Branch K, Chen G, Caldwell J, Kinahan P. Cine CT for attenuation correction in cardiac PET/CT. J Nucl Med 2007;48(5):794–801.
19. Ho CY, Wu TH, Mok GS. Interpolated average CT for PET attenuation correction in different lesion characteristics. Nucl Med Commun 2016;37(3):297–306.
20. Ai H, Pan T. Feasibility of using respiration-averaged MR images for attenuation correction of cardiac PET/MR imaging. J Appl Clin Med Phys 2015;16(4):5194.
21. Kruis MF, van de Kamer JB, Vogel WV, Belderbos JS, Sonke JJ, van Herk M. Clinical evaluation of respiration-induced attenuation uncertainties in pulmonary 3D PET/CT. EJNMMI Phys 2015;2(1):4.
22. Conti M. Why is TOF PET reconstruction a more robust method in the presence of inconsistent data? Phys Med Biol 2011;56(1):155–168.
23. Iagaru A, Minamimoto R, Levin C, et al. The potential of TOF PET-MRI for reducing artifacts in PET images. EJNMMI Phys 2015;2(Suppl 1):A77.